

New Trends in Cyclotrons

Uwe Trinks

Technische Universität München
D-85748 Garching, Germany

Abstract

Recent proposals for accelerator driven nuclear power plants demand for 1 GeV proton beams of 10 MW power. The accelerator has to be of low cost, high efficiency, and low beam losses to avoid activation problems. A separated orbit cyclotron with superconducting channel magnets and rf-cavities would meet the requirements in optimal way. The distinguishing feature of this type of cyclotron is the strong transverse and longitudinal focusing. After a general discussion of design aspects the status of the *Tritron* project is given, a small prototype with a maximum energy of 74 MeV for protons, which presently is taken into operation in *Munich*.

1 INTRODUCTION

In the early 1930s *E.O. Lawrence and M.S. Livingston* constructed the first cyclotron for 1.2 MeV Protons. Since then new ideas and improved technology resulted in powerful systems. At *PSI-Villigen* 590 MeV protons with a current of 1 mA corresponding to 0.6 MW beam power are observed, with beam losses at the extraction of 3×10^{-4} respectively 300 nA. Recently cyclotrons for 1 GeV protons and 10 MW beam power became of special interest [1]. The protons shall bombard nonfissile Th^{232} , leading to fissile U^{233} and enough neutrons to sustain fission. By this some problems of nuclear power plants shall be reduced or eliminated: the chance for dangerous accidents, the production of long-living radioactive waste and of weapons-grade materials. Two important design features for the accelerator system have to be observed. First low investment and operation costs resp. high efficiency are needed. Secondly beam losses especially at high energy (>100 MeV) cause activation, which restricts hands-on maintenance strongly. From *LAMPF* it is known, that proton losses of 1 nA/m at 800 MeV in copper correspond to a dose rate of 0.2 mSv/h at ~ 50 cm distance from the beam axis after one day delay.

The ambitious purpose could become the most important application of cyclotrons in future. Linacs, if not folded, would produce much more expenses for buildings and shielding. A repeatedly folded linac with multiple, efficient use of the cavities is at last a cyclotron. To meet the challenge, one can try to push the limits of the present state of the art cyclotron by at least an order of magnitude with regard to the beam power, and by a factor of 1.7 with respect to the energy. In view of the prospects however it appears more favourable to look for a new design with fur-

ther capability of development by using new technology. As starting point the present cyclotron design shall be examined critically. In principle an alternative solution was proposed already more than 30 years ago, known as separated orbit cyclotron (*SOC*). However to put this idea into action superconductivity was needed for bending, focusing and acceleration. Presently the first completely superconducting *SOC* is taken into operation (*Tritron*).

2 WEAK POINTS OF CONVENTIONAL CYCLOTRONS

All cyclotrons are dominated by the magnetic system. The height of the magnets always is large compared to that of the field volume really needed for bending and focusing. Since the magnetic flux is returned outside of the extraction radius the magnets become big, occupying valuable space. The rf-acceleration system and the injection / extraction elements are squeezed into narrow gaps, limiting the maximum rf-voltage respectively the turn separation and thus the beam current at extraction.

To get the revolution frequency f_{rev} independent of the velocity v of the particles (isochronism), the average bending field per turn has to increase in proportion to the relativistic mass increase γ , imposing a particular radial dependence on this field. This condition restricts the focusing power strongly. It causes the number of radial betatron oscillations to be approximately equal to γ , so that stopbands have to be crossed. The focusing power in axial direction has to be produced mainly by an azimuthal field variation, which for increasing particle energy reduces the efficiency of the bending field more and more. The problem behind all is, that the fields at neighbouring orbits are linked.

The condition of isochronism excludes longitudinal focusing. If the particles depending on their phases gain different energies in the accelerating field, these differences accumulate and cause a radial beam broadening. The lack of longitudinal focusing is a basic weakness of the ordinary isochronous cyclotron.

3 THE PRINCIPLE OF THE SEPARATED ORBIT CYCLOTRON

To overcome the problems, *F.M. Russell* proposed already in 1963 the principle of the separated orbit cyclotron (*SOC*) [2]. In a *SOC*, the particles are guided by magnetic structures along a fixed spiral path with a turn separation much bigger than the radial beam width, so that each of

the field levels and radial gradients of radially neighbouring structures can be chosen more or less independently, incorporating strong transverse focusing as in a synchrotron. The betatron oscillation numbers can be chosen far from the stability limits, resonances can be avoided. Injection and extraction is straight forward. Hence several rings can be coupled.

The particles are accelerated by rf-cavities interspersed with the sectors of the magnetic structures. The spiral path is designed in such a way, that the path length between succeeding cavities increases monotonely. The velocity of the particles has to increase correspondingly, at least on average, to keep them in phase with the accelerating voltage. For this the effective accelerating voltage per turn has to exceed a minimum voltage given by:

$$\Delta V = \frac{m_0 c^2}{e} \cdot \beta^2 \cdot \gamma^3 \cdot \frac{\Delta r_0}{r_0} \quad (1)$$

Here r_0 is the mean orbit radius (turn length over 2π) and Δr_0 its increment per turn, the mean turn separation. The particles will follow automatically particular phase curves fixed by the initial energy and phase, so in fact the revolution frequency averaged along several turns stays constant [3]. Locally the revolution frequency varies periodically due to longitudinal focusing. The relative variation of f_{rev} is given by the variations of the velocity and of r :

$$\frac{\Delta f_{rev}}{f_{rev}} = \frac{\Delta v}{v_0} - \frac{\Delta r}{r_0} \quad (2)$$

v_0 is the velocity of a hypothetical isochronous particle running along the design orbit, that is with $\Delta r = 0$ and $\Delta v = 0$. If the bending field levels of all magnetic structures are set properly –starting with the first one and continuing step by step along the spiral path with the aid of beam position probes– then the central particle of the bunch will move along the orbit without radial deviations, that is $\Delta r = 0$. However the energy of the central particle may differ from the isochronous energy, so that $\Delta v \neq 0$. The resulting frequency deviation according to Eq.(2) will lead to stationary coherent energy and phase oscillations of the whole bunch with respect to the hypothetical particle moving isochronously, if the slope of the accelerating voltage as function of the phase is positive. Noncentral particles with $\Delta r \neq 0$ will execute incoherent synchrotron oscillations with respect to the centre of the bunch. Due to the difference concerning the Δr – term in Eq.(2) the incoherent oscillation number is somewhat less than the coherent one. In the conventional isochronous cyclotron the field is chosen such that the terms on the right hand side of Eq.(2) cancel out each other. Then the particles are not fixed longitudinally.

The advantages are caused basically by the enhanced accelerating voltage per turn given by Eq.(1). Fig.1 shows $\Delta V \sim \beta \cdot \gamma^3$ as function of β , where $\beta \sim r$. Note the steep increase above $\simeq 1$ GeV, which finally makes the energy gain on the last turn to exceed that of all previous turns together. In Eq.(1) the quantity $m_0 c^2 \beta^2 \gamma^3 / e = 6.33$ GV for 1 GeV protons does not depend on the cyclotron type,

only $\Delta r_0 / r_{0ex}$ does. Δr_0 will be of the order of several cm in a *SOC* instead of some mm in conventional cyclotrons. The resulting enhancement factor can be lowered somewhat by increasing the extraction radius r_{0ex} , which favours low magnetic fields. Typically $\Delta r_0 / r_{0ex}$ is 0.012 for 1 GeV protons, giving for the accelerating voltage on the last turn 76 MV, so that some tens of cavities will be needed along the circumference of the machine, and the spiral path will consist of some tens of turns. When dealing with a beam power of 10 MW a cavity number of the order of 50 would be by no means of disadvantage, because then the power per cavity transferred to the beam is only about 200 kW and can be handled routinely.

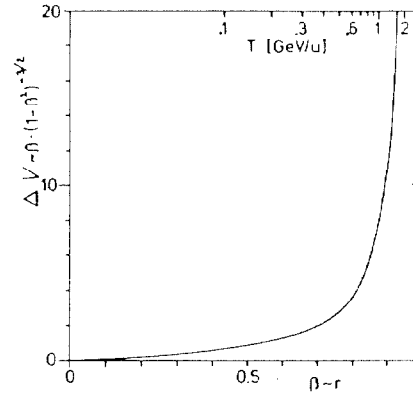


Figure 1: The dependence of $\beta \cdot \gamma^3 \sim \Delta V$ on $\beta \sim r$.

Immediately after the principle of the *SOC* had been invented, strong activities started at different places. Several systems were investigated by means of prototypes for magnets and cavities [4]. However in 1969 the work on *SOCs* was stopped. One reason may have been, that the magnets and cavities were designed according to the technology of those days, which was not any more adequate to fit the new requirements. Only with superconductivity full use can be made of the advantages of the *SOC*. However at that time superconductivity was not yet well established.

4 SUPERCONDUCTING SOC'S

In 1983 the *SOC* was proposed again, starting with the design of superconducting magnets [5]. The high current density of superconducting cables makes possible the use of channel magnets, consisting of narrow cable beams on the left and right of the particle beam within a cold rectangular channel of steel (windowframe type). Fig.2 shows a radial cross section of two combined channels for neighbouring orbits of the spiral path. If the magnetization stays below saturation (say $B \leq 1.9$ T) the ampere–turns of the coils per mm height of the window is less than 1510 A/mm, corresponding to a cable width of 3 mm at an overall current density of $\simeq 500$ A/mm. The magnetic flux between the two cable beams in the window is returned immediately in the adjacent steel frame. A radial field gradient can be imposed by two separate windings with different distances

from the central plane on the left and right side. The copper pipe supports and shields the coils. With $\Delta r_0 = 10$ cm and $B_{max} = 1.75$ T the radial aperture would be ≈ 43 mm. The axial aperture could easily be made somewhat larger, restricted only by the fact, that the stray field at the cavities has to stay $\leq 10^{-4}$ T for rf-superconductivity. All channel magnets of a sector can be combined to a sheet of magnets with a total height of about three times the gap height. Thus the cavities can be optimized with respect to peak fields and wall losses.

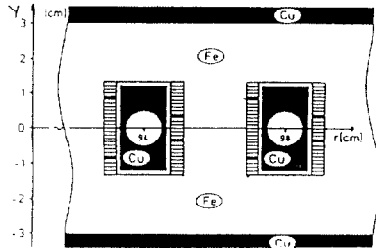


Figure 2: Radial cross section of two channel magnets.

The optimal shape of the accelerating cavity is a big sector, with the lateral walls inward directed in the central region, where the particles enter and leave the cavity, forming radially extended accelerating lips (see Fig. 3). The gap width increases linearly. Into the lateral caves outside of the accelerating gap the magnet sectors can be inserted.

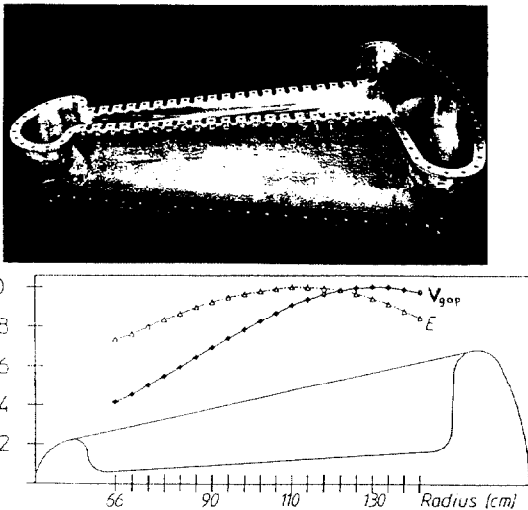


Figure 3: Lower half of a cavity of optimized shape ($f_{rf} = 170$ MHz, length 1.23 m, gap width at injection 62 mm, at extraction 128 mm).

Due to the size the frequency is rather low, so that the gap width can be chosen large without loosing at the transit time factor. The electrical peak field E_{peak} limits the maximum gap voltage due to field emission. In contrast to other types of cavities all radii of curvature can be chosen sufficiently large, so that a rather low value $E_{peak}/E_{acc} \leq 1.5$ can be achieved. The dissipated heat in the cavity walls per voltage gain of the particles can be

written as

$$\frac{P_{wall}}{V} = \frac{V_{max}^2}{2 \cdot n \cdot V_{ave} \cdot R_{sh}} = \frac{V_{max}^2 \cdot R_s}{2 \cdot n \cdot V_{ave} \cdot G \sqrt{L}} \quad (3)$$

with R_{sh} the shunt impedance, R_s the surface resistance of the wall, n the number of beam holes per cavity, V_{max} the maximum and V_{ave} the average gap voltage, L the effective inductance, C the effective capacitance, and G the geometry factor, which is independent of the frequency and is maximum for spherical cavities ($\approx 300\Omega$) and low for quarter-wave cavities ($\approx 20\Omega$). Eq.(3) shows, that L should be made as large as possible, thus keeping the magnetical surface fields relatively small. The cavity shown in Fig.3 has $G \approx 90\Omega$, and $\sqrt{L/C} \approx 60\Omega$.

Though this cavity is of rather optimal shape, the specific losses would be as high as $P_{wall}/V \approx 8$ mW/V, if the cavity would be made from Cu with $R_s \approx 3.4$ m Ω (with $n = 20$, $V_{max} = 700$ kV and $V_{ave} = 500$ kV). For 1 GeV protons the total wall losses would be ≈ 8 MW. This number can be reduced by a factor of $\approx 10^{-4}$, if the cavity would be superconducting. Even if the effective cryogenic efficiency for removing the wall losses at the temperature of 4.2 K is assumed to be 1/500, the gain factor for the power would be 20, and the effective dissipated power for the rf-system would be small compared to a beam power of 10 MW.

The wall losses in superconducting cavities are caused by the normal conducting electrons, being accelerated by the rf fields in a thin surface layer. R_s consists of R_{BCS} from the BCS-theory and the temperature independent residual resistance R_{res} . R_{BCS} is approximately proportional to f_{rf}^2 and goes down with decreasing temperature. To R_{res} contribute normal conducting spots and dielectrics on the surface. Fig.4 shows the frequency dependence of the BCS surface resistance of Pb, PbSn (4 Sn, 96 Pb atoms), and Nb at 4.2 K [6]. The critical temperatures are for Pb: 7.2 K, PbSn: 7.5 K, and Nb: 9.2 K.

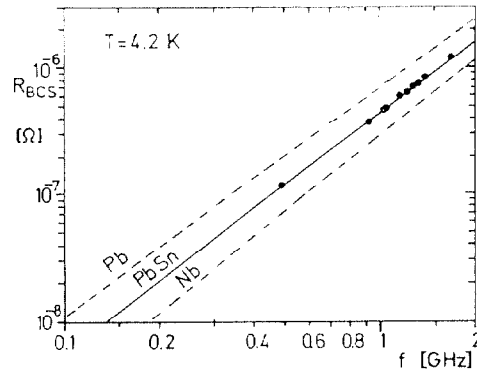


Figure 4: Frequency dependence of R_{BCS} of Pb, PbSn (96/4), and Nb at 4.2 K.

At the rather low frequencies of the big cavities discussed here the surface resistance is extremely low. This has important technical consequences. First the cavities can be operated at a temperature of about 4.5 K. Secondly niobium as superconductor is not needed. Cavities made

from Nb sheets would be rather expensive and demand for complicated bath cooling. The sputtering technique is not yet established for cavities without rotational symmetry, at least not for cavities of the size and shape needed here. In contrast to Pb or PbSn it is not possible either to electroplate Nb onto copper. PbSn is superior to Pb, because it has a better throwing power during the electroplating procedure, PbSn is chemically more stable, and it is a somewhat better superconductor. The thickness of the layer needs not to be more than $\approx 2\mu\text{m}$. The dissipated heat will be drained off by the copper walls (some cm thick, produced by the electroforming technique), so that indirect pipe cooling can be applied. The amount of liquid helium is kept small. It is easy to install couplers and frequency tuning equipments [9].

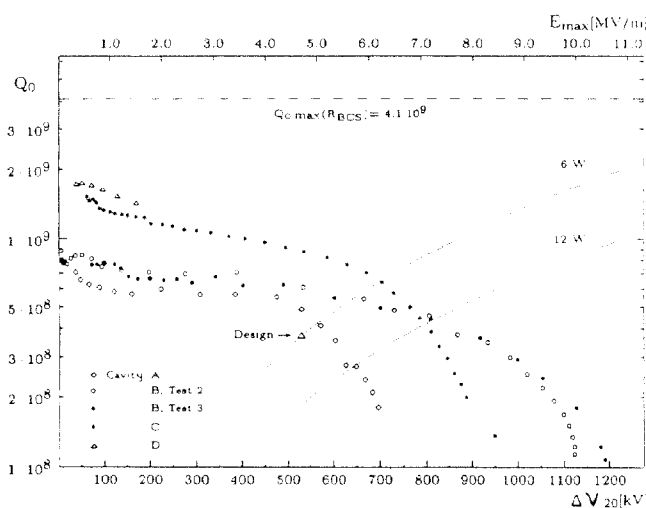


Figure 5: Unloaded quality factor Q_0 versus the voltage V_{20} resp. the maximum gap field.

In Fig.5 some measurements of the Q_0 -values versus the gap voltage at the last (20th) beam hole resp. the maximum gap field E_{max} at the 13th beam hole are shown ($T \leq 5\text{ K}$, background induction $\leq 5 \cdot 10^{-5}\text{ T}$) for some cavities as shown in Fig.3. The cavities were electroplated with the PbSn-layers in alphabetic order. The improvement of the later Q -values indicates the progress in the surface preparation technique. The dotted curves are for constant dissipated heat. The broken line gives the theoretical upper limit.

Up to now the quality factor showed no degradation during several months, though the cavities were exposed to air many times. This good results in spite of the large total surface of $\approx 3\text{m}^2$ per cavity can be explained by the fact, that the heat, dissipated in small normal-conducting spots e.g., will be lead away from the thin PbSn layer into the copper body very effectively, causing a rather small temperature increase and preventing the spots to grow, at least below a certain maximum power input. In addition the skin depth of the rf-fields in normal-conducting PbSn exceeds the thickness of the layer considerably.

5 THE TRITRON PROJECT

Based on the preceding design considerations a rather small machine was developed at Munich, the *Tritron* (Fig.6). In Tab.1 some data are summarized [5,..11]. The main purpose of this machine was to develop the superconducting channel magnets and cavities and to gain experience in the design and operation of this new type of accelerator. When the project was started it was unknown, if superconducting cavities as shown in Fig.3 would operate at all. In order to keep the accelerating voltage per turn low (design: 3.2 MV on the last turn), the turn separation respectively the width of the channel magnets were chosen as small as possible: $\Delta r_0 = 40\text{ mm}$ (see Fig.2). Due to the resulting small aperture of the magnets ($d = 10\text{ mm}$) the machine will not be suited to accelerate beams with high currents.

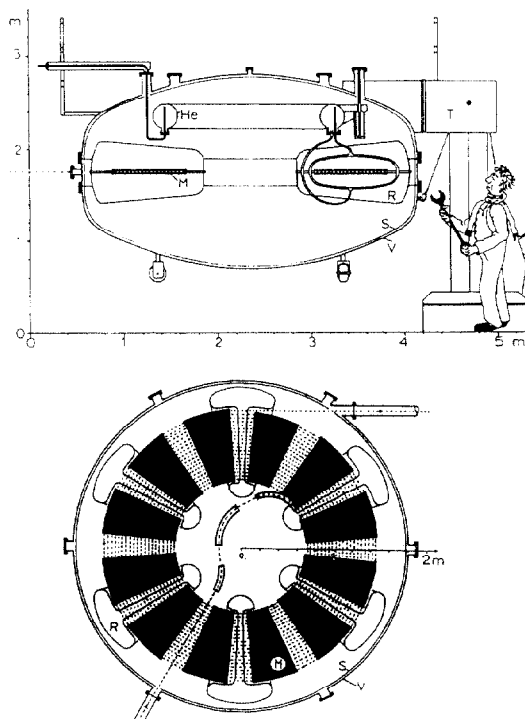


Figure 6: Vertical cross sections of the *Tritron* cryostat.

Neighbouring channel magnets are combined to 12 flat sectors. In each second of the intermediate sectors a superconducting rf-cavity is inserted, operated at fixed frequency. In the remaining free sectors beam position probes for both coordinates are installed in front of each channel magnet. In total 60 small superconducting steerer magnets provide for axial beam corrections.

The cryostat consists of two shells with a diameter of 3.6 m, the upper half is held by three supports, the lower half can be removed. All feeders are installed on the upper half. The cavities and magnet sectors are hanging on a torus-shaped liquid helium reservoir (total volume 0.27 m³). To the reservoir are cooling pipes connected for the indirect thermal siphon cooling system of the magnets and cavities. To cool down from 300 K to $\approx 4.5\text{ K}$ helium gas is forced to flow through a second pipe system connected

in series with heat exchangers in the refrigerator. A radiation shield cooled by liquid nitrogen is installed on the inside of the cryostat some cm away from the wall. The insulating vacuum of the cryostat is the same as for the beam, there is no separate vacuum chamber.

Table 1: General design data of the *Tritron*

Injector	MP-tandem (14MV)
Energy gain factor	≈ 4.9
Injection radius	0.66 m
Extraction radius	1.45 m
Turn separation	40 mm
Number of turns	19.8
<i>magnet data:</i>	
Number of magnet sectors	12
Number of channel magnets/sector	20 (19)
Bending angle per channel	30°
Sector angle	20°
Bending radius ρ_1, ρ_2	430 mm, 942 mm
Geometrical aperture	10 mm
Maximum magnetic induction	
sector channels	1.7 T
3 rd injection channel	2.4 T
Normal radial gradients $\frac{\partial B}{\partial r} \cdot \frac{1}{B}$	3.6 m ⁻¹ , - 4.9 m ⁻¹
Betatron oscillation numbers Q_x	1.2 ... 1.6
Q_y	0.8 ... 1.7
Synchrotr. oscill. numbers (incoh.)	≈ 0.2
<i>cavity data:</i>	
Number of cavities	6
Fixed rf-frequency	170 MHz
Harmonic numbers	$\approx 14 - \approx 55$
Total radial length	1233 mm
Radial gap length	≈ 0.85 m
Gap width injection/extraction	62 mm / 128 mm
Aperture of the beam holes	13 mm
Maximum gap voltage	0.53 MV
Maximum accelerating field	4.7 MV/m
Peak field to maximum gap field	< 1.5
Unloaded quality factor	$3.7 \cdot 10^8$
Dissipated power per cavity	6 W
Surface resistance	$2.5 \cdot 10^{-7} \Omega$

Representative field measurements with good results were made on some 50 channel magnets. Four cavities have been conditioned so far and exceed the design values. The assemblage of all parts inside the vacuum vessel was finished at the beginning of 1994. The cryosystem including the refrigerator (155 W at 4.6 K) is operating well. Evacuation of the cryostat needs about 30 h (to achieve $\approx 5 \cdot 10^{-2}$ Pa). Then cooling of the in total 7 tns is started. It takes about 90 h to reach superconductivity. The stand-by load on the 4.5 K level is less than 50 W, the consumption of liquid nitrogen is less than 25 l/h. Due to the good cryopumping the pressure in the cryostat generally is less than or about 10^{-5} Pa. Heating from 4.5 K to room temperature and pressurizing the vacuum vessel with N₂ gas takes ≈ 50 h. A complete cycle evacuation - cooling - heating - pressurizing takes ≈ 7 days. The beam guiding system from the tandem to the Tritron is ready except of the bunching system. The computer control system of the tandem and Tritron is in an advanced state. First beams passed successfully through the three injection channels, the following five channel magnets as well as three cavities on half of the innermost turn. No influence of stray-fields on the cavities were observed. When operating the first cavity at rather high levels, the expected horizontal spread

of the unbunched beam was observed downstream. All channel magnets were operating at the same time with currents up to 1000 A (about 60% of maximum). The technique of individual current setting in the channels by just one power supply by means of superconducting bypass switches was tested successfully. The fields in the three injection channels and the following five, innermost channels with the switch superconducting stayed stable, when the current in the switches was changed by ± 100 A. No effect on the beam position was observed. In total 6 of some 120 beam probes (wire scanners) were operating under real conditions with good results. The first superconducting steerer magnets for axial beam corrections were taken into operation.

The commissioning of the whole accelerator system is going on step by step.

6 ACKNOWLEDGEMENTS

Thanks are given to all members of the *Tritron* group. Work funded by the *German Federal Minister for Research and Technology (BMFT)* under the contract 06 TM 189.

7 REFERENCES

- [1] F. Carminati, R. Klapisch, J.P. Revol, Ch. Ruche, J.A. Rubbia and C. Rubbia, "An Energy Amplifier for Cleaner and Inexhaustible Nuclear Energy Production Drive by a Particle Beam Accelerator", CERN / AT / 93-47 (ET).
- [2] F.M. Russell, "A Fixed-Frequency, Fixed-Field, High-Energy Accelerator", Nucl.Instr.Meth., vol. 23, p. 229, 1963.
- [3] U. Trinks, "Longitudinal Particle Dynamics in the Tritron", Nucl.Instr.Meth., vol. A306, p. 27, 1991.
- [4] J.A. Martin, "The Separated-Orbit Cyclotron", IEEE Trans. Nucl. Sci. vol. NS-13, p. 288, 1966.
- [5] U. Trinks, W. Assmann and G. Hinderer, "The Tritron: A Superconducting Separated Orbit Cyclotron", Nucl.Instr.Meth., vol. A244, p. 273, 1986.
- [6] L. Dietl, U. Trinks, "The Surface Resistance of a Supercond. Lead-Tin Alloy", Nucl.Instr.Meth., vol. A284, p.293, 1989.
- [7] G. Hinderer, C. Rieß, U. Trinks, "Transverse Beam Dynamics and Coupling Effects in the Tritron", Nucl.Instr.Meth., vol. A317, p. 13, 1992.
- [8] R. Kratz, G. Hinderer, J. Junger, J. Labedzki, U. Trinks, "The Superconducting Tritron Magnets", in 1991 IEEE Part. Accel. Conf., San Francisco, USA, May 1991, p. 2254.
- [9] T. Grundey, J. Labedzki, P. Schütz, U. Trinks, "The Supercond. Accelerating Cavities for the Tritron", Nucl.Instr.Meth., vol. A306, p. 21, 1991.
- [10] U. Trinks, "The Superconducting Separated-Orbit Cyclotron Tritron", in 13th Int.Conf.Cycltr., Vancouver, Canada, 1992, p. 693.
- [11] U. Trinks, "Exotic Cyclotrons - Future Cyclotrons", to be publ., CERN Accelerator School, LaHulpe, 1994.